Journal of Magnetic Resonance **141,** 133–140 (1999)
Article ID jmre.1999.1845, available online at http://www.idealibrary.com on IDEAL®

Determination of Coupling Constants by Deconvolution of Multiplets in NMR[1]

Damien Jeannerat* and Geoffrey Bodenhausen†,[2]

*Département de chimie, Université de Genève, 30 Quai Ernest Ansermet, CH-1211 Genève 4, Switzerland; and
†Département de chimie, Ecole Normale Supérieure, 24 rue Lhomond, F-75231 Paris Cedex 05, France

Received March 22, 1999; revised June 10, 1999

The structures of multiplets in one- and two-dimensional NMR spectra can be simplified by recursive deconvolution in the frequency domain. Deconvolution procedures are described for in-phase and antiphase doublets of delta functions. Recursive simplification is illustrated by applications to double-quantum-filtered correlation spectra (DQF-COSY) and selective correlation spectra (soft-COSY). Coupling constants can be measured reliably even if signals of opposite signs lead to partial cancellation.

Key Words: **deconvolution of multiplets; correlation spectroscopy (COSY); cross-peak multiplets.**

The structure of multiplets in one- and two-dimensional NMR spectra contains a wealth of information about scalar and dipolar couplings. The coupling constants can be determined by deconvolution in the frequency or in the time domain (*1–3*), by maximum entropy techniques (*4–6*), or by taking advantage of properties of trigonometric functions (*7*). In this paper, we shall focus on frequency-domain analysis (*8*), pursuing the work by Huber and Bodenhausen (*9*). Some of the difficulties encountered in determining the inverse of convolution have been overcome and the criteria for the success of simplification have been improved.

The convolution product of two functions f and g may be defined as follows:

$$h(x) = \int_{-\infty}^{\infty} f(u)\, g(x-u)du. \qquad [1]$$

If the functions are discrete, the integral may be replaced by a sum. Thus, convolution of two arrays $\boldsymbol{a} = \{a_0, a_1, \ldots, a_n\}$ and $\boldsymbol{b} = \{b_0, b_1, \ldots, b_m\}$ gives an array $\boldsymbol{c} = \{c_0, c_1, \ldots, c_{n+m}\}$ containing $n + m + 1$ elements, where

$$c_i = \sum_{k=0}^{i} a_k b_{i-k}. \qquad [2]$$

We shall refer to the operation which allows one to derive the array $\boldsymbol{a}$ from the knowledge of $\boldsymbol{b}$ and $\boldsymbol{c}$ as *deconvolution.* As shown by Bracewell (*10*), this can be expressed as

$$a_k = b_0^{-1}(c_k - \sum_{j=0}^{k-1} a_j b_{k-j}). \qquad [3]$$

This equation can be verified by substitution into Eq. [2]. We shall only consider multiplets that are composed of in-phase and antiphase doublets. An in-phase doublet of delta functions can be represented by an array $\boldsymbol{b}$,

$$b_i = \begin{cases} +1, & i = 0 \\ +1, & i = m \\ 0, & \text{elsewhere} \end{cases} \qquad [4]$$

and an antiphase doublet by another array $\boldsymbol{b}$,

$$b_i = \begin{cases} +1, & i = 0 \\ -1, & i = m \\ 0, & \text{elsewhere.} \end{cases} \qquad [5]$$

For such doublets, Eq. [3] can be simplified since there is only one nonzero element in the summation, so that we obtain for in-phase doublets,

$$a_k = c_k - a_{k-m}, \qquad [6]$$

and for antiphase doublets,

$$a_k = c_k + a_{k-m}. \qquad [7]$$

Thus each point of the deconvoluted spectrum can be computed by taking the sum or difference of only two numbers. In the case of in-phase doublets we obtain

[1] This work was carried out in part at the Center for Interdisciplinary Magnetic Resonance, National High Magnetic Field Laboratory, 1800 East Paul Dirac Drive, Tallahassee, FL 32310.

[2] To whom correspondence should be addressed. Geoffrey.Bodenhausen@ens.fr.

1090-7807/99 $30.00

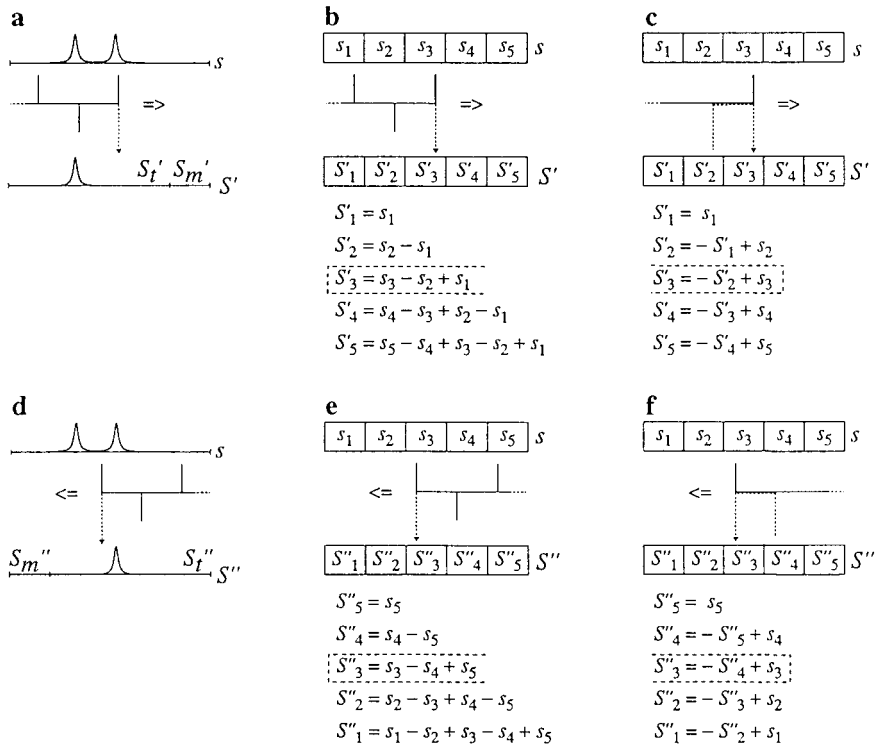

FIG. 1. (a) Simplification of an in-phase doublet by asymmetrical deconvolution from left to right. The deconvoluted spectrum $\boldsymbol{S'}$ can be separated into a segment $\boldsymbol{S}'_t$ that contains the simplified spectrum and a *marginal domain* $\boldsymbol{S}'_m$ that should not contain any signals if deconvolution is successful. (b) Deconvolution according to Eq. [8]. (c) Deconvolution according to the recursive formula of Eq. [6]. Note that the two approaches are equivalent. (d–f) Deconvolution obtained by moving the array $\boldsymbol{a}$ from right to left.

$$a_k = c_k - c_{k-m} + c_{k-2m} - c_{k-3m} \cdots = \sum_{i=0}^{p} (-1)^i c_{k-im}, \quad [8]$$

where $p \leq k/m$. For antiphase doublets we have

$$a_k = c_k + c_{k-m} + c_{k-2m} + c_{k-3m} \cdots = \sum_{i=0}^{p} c_{k-im}. \quad [9]$$

For the in-phase case, Eq. [8] can be rewritten,

$$a_k = \sum_{i=0}^{k} d_i c_{k-i}, \quad d_i = \begin{cases} 1, & i = 0, 2m, 4m, 6m, \ldots \\ -1, & i = m, 3m, 5m, \ldots \\ 0, & \text{elsewhere,} \end{cases} \quad [10]$$

while for the antiphase case of Eq. [9] we obtain

$$a_k = \sum_{i=0}^{k} d_i c_{k-i}, \quad d_i = \begin{cases} 1, & i = 0, m, 2m, 3m, \ldots \\ 0, & \text{elsewhere.} \end{cases} \quad [11]$$

Thus the deconvolution of in-phase multiplets can be achieved with an array $\boldsymbol{d}$ that has the form of a series of delta functions with alternating signs $[+ - + - \cdots]$ separated by a distance m. This spacing m corresponds to the trial value J^* of the (as yet unknown) splitting. Deconvolution of antiphase multiplets requires a series of delta functions with the same signs $[+ + + + \cdots]$, also separated by a distance m. Note that, although the array $\boldsymbol{a}$ only comprises $n + 1$ elements, Eqs. [10] and [11] yield an infinite array $\boldsymbol{d}$. The deconvoluted spectrum may be expressed as

$$S'_k = \sum_{i=0}^{k} d_i s_{k-i}, \quad [12]$$

where $\boldsymbol{s}$ represents an experimental spectrum with $n + m + 1$ elements and $\boldsymbol{d}$ is one of the infinite arrays of delta functions defined above. If the trial splitting J^* corresponds to a true J splitting in the spectrum, the resulting array $\boldsymbol{S'}$ should have a simplified structure in comparison with the original spectrum $\boldsymbol{s}$. For any value of J^*, the last m elements will be called the *marginal part* $\boldsymbol{S}'_m$ while the beginning of the array $\boldsymbol{S'}$ will be referred to as *truncated array* $\boldsymbol{S}'_t$. If deconvolution is successful and leads to a simplified structure, $\boldsymbol{S}'_m$ should contain only zeroes, as illustrated in Fig. 1a. The raw spectrum $\boldsymbol{s}$ is convoluted with an array $\boldsymbol{d}$ defined in Eq. [10], which is moved from

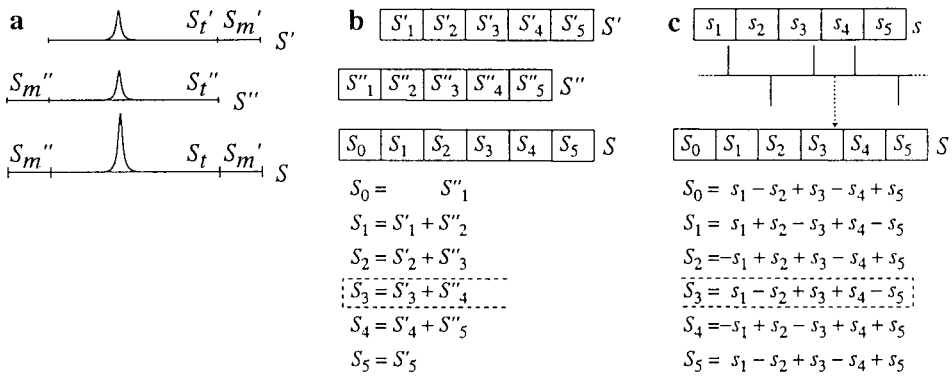

FIG. 2. (a) Shifting and summation of deconvoluted spectra $\boldsymbol{S'}$ and $\boldsymbol{S''}$, resulting in $\boldsymbol{S}$, which can be separated into a central segment $\boldsymbol{S}_t$ that contains the simplified spectrum, and two *marginal domains* $\boldsymbol{S}'_m$ and $\boldsymbol{S}''_m$ that should not contain any signals if deconvolution is successful. (b, c) Schemes highlighting the equivalence of the asymmetrical and symmetrical approaches to deconvolution.

left to right with respect to the spectrum, so that the product can be calculated point-by-point. At the beginning of the process, $\boldsymbol{s}$ is simply copied into $\boldsymbol{S'}$. The further the array of delta functions moves to the right, the larger the number of points belonging to $\boldsymbol{s}$ which affect the resulting array $\boldsymbol{S'}$. Artifacts and noise will therefore be amplified from left to right. The smaller the splitting J^*, the closer the spacing between the delta functions in the array $\boldsymbol{d}$, and the more the artifacts are amplified in $\boldsymbol{S'}$. To reduce these artifacts to a minimum, we limit deconvolution to a narrow spectral window that contains the signal. When multiplets have complex structures, the best results will be obtained for deconvolution of the largest splitting. We shall see later that this approach has other advantages.

When the deconvolution process is started from the right-hand side of the spectrum (*11*), the artifacts and noise increase from right to left (see Figs. 1d–1f). We shall use double primes to label arrays obtained in this way. As shown in Fig. 2, the arrays $\boldsymbol{S'}$ and $\boldsymbol{S''}$ have to be displaced relative to each other prior to summation (*11*). If deconvolution is successful (i.e., when $J^* = J$) this displacement should be equal to J^*, as shown in Fig. 2. In the case of deconvolution of antiphase doublets, the sign of $\boldsymbol{S''}$ has to be inverted before summation.

Figure 3 illustrates the different approaches. The amplitudes of the waves are proportional to the number of contributions and thus to the amplitude of artifacts and noise. It is apparent that $\boldsymbol{S}$ has a uniform amplitude across the entire spectrum since each point is made up of the same number of contributions. This approach will be our method of choice unless specified otherwise. Figure 3d was obtained by combining the best parts of $\boldsymbol{S'}$ and $\boldsymbol{S''}$. This alows one to minimize noise and artifacts, but has the disadvantage of introducing a discontinuity between the two halves of the multiplet.

In a private communication, Bothner-By proposed (*12*) to use an infinite array of delta functions [$\cdots - + - + + - + - \cdots$] to deconvolute in-phase doublets. Likewise, antiphase doublets can be deconvoluted by an infinite array [$\cdots + + - - - \cdots$]. It turns out that the application of these methods directly leads to $\boldsymbol{S}_t$ (see Fig. 3c). This approach is formally more satisfactory (*8*), but the two-step procedure appears to be easier to implement in practice. Moreover, the latter allows one to test the symmetry of $\boldsymbol{S}'_t$ or $\boldsymbol{S}''_t$ separately (see below) to determine to what extent the simplification is successful, while $\boldsymbol{S}_t$ is not appropriate for such an analysis since it is intrinsically symmetrical.

If deconvolution is successful, it should lead to a simplification of the spectrum. The simplest way to measure the extent of simplification is to consider the sum of the absolute values of all points of $\boldsymbol{S'}$ (*9*), which will be called the *global integrated absolute value* Abs($\boldsymbol{S'}$):

$$\mathrm{Abs}(\boldsymbol{S'}) = \sum_{i=0}^{k} |S_i|. \qquad [13]$$

This reaches a minimum value when deconvolution is successful. In many cases, it is advantageous to limit the integration to the last m elements of $\boldsymbol{S'}$, i.e., to the *marginal* part $\boldsymbol{S}'_m$, in which case we may speak of the *marginal integrated absolute value:* Abs($\boldsymbol{S}'_m$). This should vanish if deconvolution is successful. In either case, the integrals must be computed for all trial values J^*.

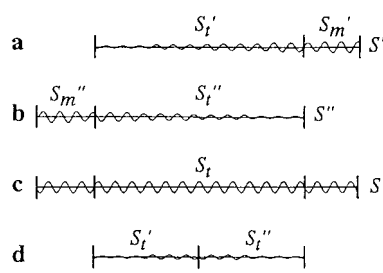

FIG. 3. Schematic representation of artifacts with increasing and decreasing amplitudes appearing as a result of deconvolution (a) from left to right and (b) from right to left. The deconvoluted segments $\boldsymbol{S}'_t$ and $\boldsymbol{S}''_t$ that contain the simplified spectrum can be distinguished from the marginal domains $\boldsymbol{S}'_m$ and $\boldsymbol{S}''_m$. (c) Spectrum obtained by symmetrical deconvolution. The central region $\boldsymbol{S}_t$ is equal to the sum of $\boldsymbol{S}'_t$ and $\boldsymbol{S}''_t$. (d) Juxtaposition of the first half of $\boldsymbol{S}'_t$ and the second half of $\boldsymbol{S}''_t$.

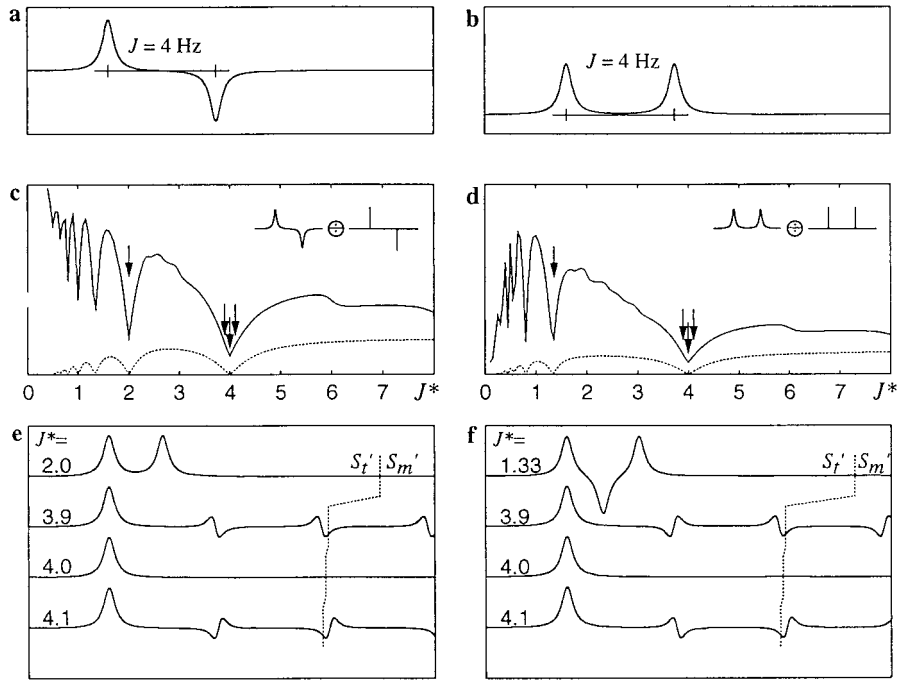

FIG. 4. (a) Simulated antiphase doublet and (b) in-phase doublet, both with a true splitting $J = 4$ Hz and a linewidth at half-height of 0.5 Hz. (c) Global integrated absolute value Abs($\boldsymbol{S}'$) of Eq. [13] (continuous line) and marginal integrated absolute value Abs($\boldsymbol{S}'_m$) (dotted line) calculated after deconvolution of the antiphase doublet in (a) with antiphase doublets of delta functions as a function of the trial splitting J^*. The first minimum from the right of both absolute value functions in (c) gives the correct coupling constant $J^* = J = 4$ Hz. Arrows indicate four values of J^* for which the deconvoluted spectra are shown in (e). The vertical dotted lines in (e) indicate the limits between the $\boldsymbol{S}'_t$ and $\boldsymbol{S}'_m$ domains. When $J^* \neq J$, residual antiphase features appear in (e). Note the appearance of misleading secondary minima in (c) for submultiples $J^* = J/n$. (d) Global integrated absolute value Abs($\boldsymbol{S}'$) (continuous line) and marginal integrated absolute value Abs($\boldsymbol{S}'_m$) (dotted line) calculated after deconvolution of the in-phase doublet (b) with in-phase doublets of delta functions separated by J^*. The first minimum from the right of both functions in (d) gives the correct coupling constant $J^* = J = 4$ Hz. Arrows indicate values of J^* for which the deconvoluted spectra are shown in (f). The vertical dotted lines in (f) indicate the limits between the $\boldsymbol{S}'_t$ and $\boldsymbol{S}'_m$ domains. Note the presence of secondary minima in (d) for odd submultiples $J^* = J/(2n + 1)$.

Figure 4 shows some simulated examples of deconvolution of in-phase and antiphase doublets. The global and marginal functions Abs($\boldsymbol{S}'$) and Abs($\boldsymbol{S}'_m$) are drawn with plain and dotted lines in Figs. 4c and 4d. For an antiphase splitting, the marginal function Abs($\boldsymbol{S}'_m$) vanishes for $J^* = J$ and for submultiples $J^* = J/n$. The global function Abs($\boldsymbol{S}'$) merely shows minima at these positions. The lowest minimum corresponds to the correct splitting. However, simply taking the lowest point of the function is fraught with danger, especially when the spectrum has several splittings. Moreover, the linewidth affects the outcome. For an in-phase splitting, minima appear not only for the true splitting $J^* = J$, but also for odd subharmonics $J^* = J/(2n + 1)$.

Figure 5 illustrates what happens if one attempts to deconvolute an antiphase splitting with in-phase delta functions and vice versa. If one searches for antiphase structures in a spectrum that contains only an in-phase doublet, one does not encounter any disturbing properties (*8*). The reverse situation must however be considered with caution, as can be appreciated in Fig. 5a.

As an alternative to integrated absolute value functions, the success of deconvolution of multiplets can be ascertained using symmetry properties. Prior to symmetry mapping, the mul-

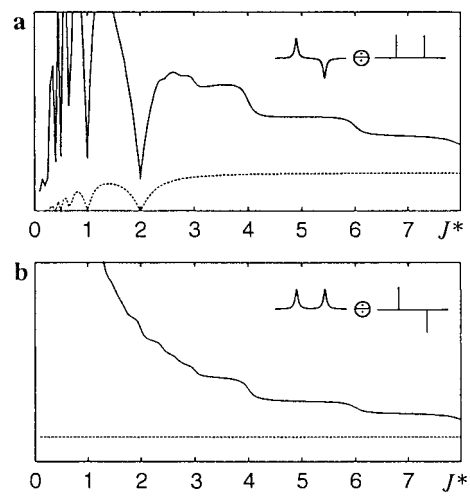

FIG. 5. (a) Global integrated absolute value Abs($\boldsymbol{S}'$) (continuous line) and marginal integrated absolute value Abs($\boldsymbol{S}'_m$) (dotted line) calculated after attempting to deconvolute the antiphase doublet of Fig. 4a by an in-phase doublet of delta functions. Misleading minima appear at even submultiples $J^* = J/(2n)$. (b) Functions Abs($\boldsymbol{S}'$) (continuous line) and Abs($\boldsymbol{S}'_m$) (dotted line) calculated after attempting to deconvolute the in-phase doublet of Fig. 4b by an antiphase doublet of delta functions. No misleading responses appear in this case.

tiplets must be phased correctly and their centers identified and moved to the center of the window using appropriate symmetry criteria (*8*). Deconvolution is then carried out using Eq. [3]. The deconvoluted structure can be compared with its symmetry-related image using a normalized scalar product $\boldsymbol{P}$ which for an n-dimensional vector $\boldsymbol{R}$ is defined by

$$\boldsymbol{P} = \frac{\sum_{i=0}^{n-1} R_i R_{(n-i)}}{\sqrt{\sum_{i=0}^{n-1} R_i^2 \cdot \sum_{i=0}^{n-1} R_{(n-i)}^2}}. \qquad [14]$$

Two situations give rise to simplified multiplets. In the first case, $\boldsymbol{P}$ may reach $+1$ when the deconvoluted multiplet is symmetrical with respect to its center. This occurs when the simplified structure contains only in-phase doublets or when the number of antiphase splittings is even. In the second case, $\boldsymbol{P}$ reaches -1 since the signal amplitudes have opposite signs relative to the center of the multiplet. This occurs when an odd number of antiphase splittings is present. In this case, we systematically inverted the sign of $\boldsymbol{P}(J^*)$ to facilitate both visual inspection and automatic peak-picking.

Inspection of Figs. 4 and 5 shows that, when starting from the right by decreasing the trial splitting J^* from an upper limit, the first extremum corresponds to the largest splitting. The combination of in-phase and antiphase splittings leads to complex patterns of extrema (*8*). Their structure contains information on all remaining splittings. Although visual interpretation is often possible (see below), attemps to make the analysis of such patterns automatic ran into difficulties. In the approach we propose, only the position of the first extremum, which corresponds to the largest splitting in the multiplet, is utilized. In order to determine the other (smaller) splittings, the simplified structure is used as starting material for the next deconvolution cycle. This allows one to measure each splitting in complex multiplets in a recursive process. This approach has the additional advantage that one can improve the quality of the multiplets in each intermediate result by symmetrization.

Although the determination of the largest splitting seems to be reliable, structures containing both in-phase and antiphase doublets represent a challenge. When a cross-peak multiplet contains equal in-phase and antiphase couplings, only one

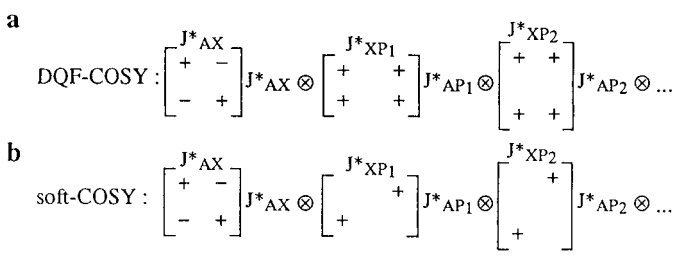

FIG. 6. Multiplet structures of (a) DQF-COSY and (b) soft-COSY cross peaks presented as convolution products of two-dimensional arrays of delta functions. The square array with alternating signs is due to the active coupling, while each passive spin gives rise to a rectangular array with an in-phase structure.

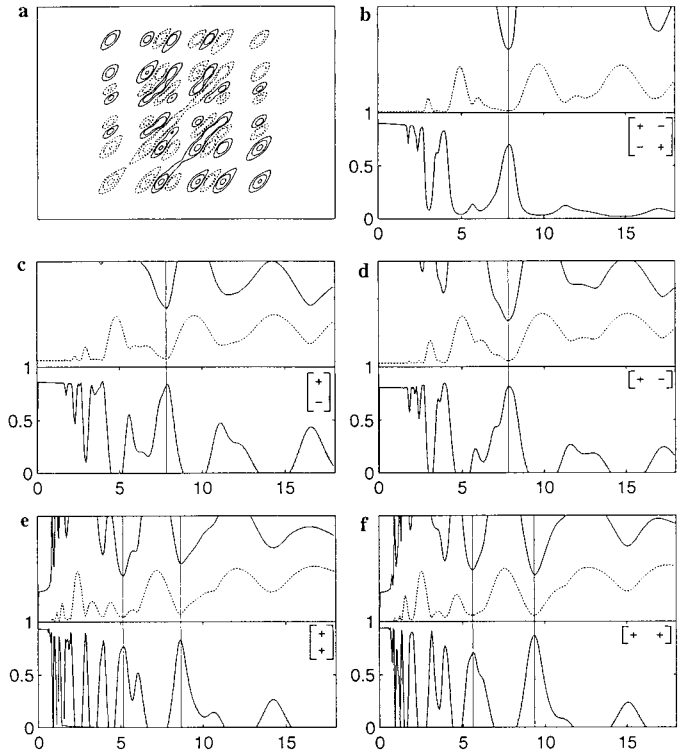

FIG. 7. (a) Experimental multiplet (32 × 45 Hz) stemming from magnetization transfer from X to M in *cis*-2-phenylcyclopropanecarboxylic acid ethyl ester (**I**), taken from a DQF-COSY spectrum with band-selective excitation. (b–f) Results of five different deconvolution procedures combined with three different criteria for the success of deconvolution. The upper halves of the frames show the global and marginal integrated absolute value functions (continuous and dotted lines, respectively). The lower halves of the frames give the symmetry of the deconvoluted multiplets. The arrays of delta functions used for deconvolution are indicated symbolically: (b) antiphase square, (c) antiphase doublet in the ω_1 dimension, (d) antiphase doublet in the ω_2 dimension, (e) in-phase doublet in the ω_1 dimension, and (f) in-phase doublet in the ω_2 dimension. The vertical lines indicate the true couplings: the active coupling is 7.85 ± 0.05 Hz in both dimensions, as can be seen in (b–d); the passive couplings correspond to 5.20 ± 0.05 and 8.65 ± 0.05 Hz in the vertical ω_1 dimension, as can be appreciated in (e), and to 5.60 ± 0.05 and 9.35 ± 0.05 Hz in the horizontal ω_2 dimension, as can be determined in (f). The vertical lines show the positions of the true splittings. The errors correspond to the half-widths at 99% of the height of the relevant peaks in the symmetry functions.

splitting corresponding to twice the coupling constant is observed. This fundamental ambiguity makes it impossible to distinguish an antiphase doublet with an apparent splitting $2J$ from two splittings J, one in-phase and one antiphase. In two-dimensional spectroscopy, this is unlikely to occur in both dimensions, but when it does, the apparent active couplings measured in the two dimensions do not match (*13*).

In order to apply deconvolution to cross peaks in band-selective versions of DQF-COSY (*14*, *15*) and soft-COSY (*16*) (see Fig. 6), it is necessary to modify the criteria for the success of deconvolution. For DQF-COSY cross peaks, deconvolution is simply applied separately to each row and column of the two-dimensional array. For soft-COSY multiplets, the search has to be conducted simultaneously in both frequency dimensions. Details are given elsewhere about the marginal integrated absolute value (*8*). To

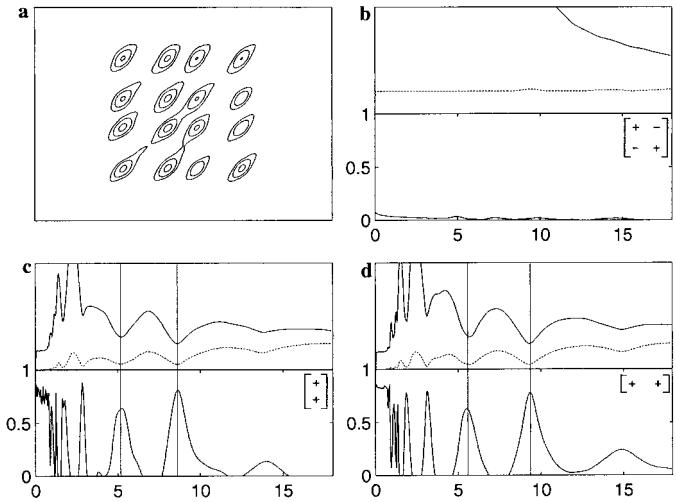

FIG. 8. (a) In-phase multiplet (27 × 37 Hz) derived from Fig. 7a after deconvolution of the active splitting with $J^* = 7.85$ Hz in both dimensions. The deconvolution was started from each of the four corners, and the results were superimposed. (b–d) Results of three different deconvolution procedures combined with three different criteria for the success of deconvolution. The upper halves of the frames show the global and marginal integrated absolute value functions (continuous and dotted lines, respectively). The lower halves of the frames give the symmetry of the deconvoluted multiplets. The arrays of delta functions used for deconvolution are indicated symbolically: (b) antiphase square, (c) in-phase doublet in the ω_1 dimension, and (d) in-phase doublet in the ω_2 dimension. As expected, no extrema can be seen in (b), since the antiphase pattern has been removed. The absolute value functions in (c) and (d) look similar to those of Figs. 7e and 7f, except that the extrema at odd submultiples of the active coupling have disappeared. The vertical lines show the positions of the true passive splittings.

obtain an accurate measure of symmetry, cross-peak multiplets first must be phased correctly and their centers must be identified (*17*). They can then be compared with their C_2 symmetry-related image using a normalized scalar product which is defined for an $n \times m$ matrix $\boldsymbol{R}$:

$$\boldsymbol{P} = \frac{\sum_{i=0}^{n-1} \sum_{j=0}^{m-1} R_{ij} R_{(n-i)(m-j)}}{\sqrt{\sum_{i=0}^{n-1} \sum_{j=0}^{m-1} R_{ij}^2 \cdot \sum_{i=0}^{n-1} \sum_{j=0}^{m-1} R_{(n-i)(m-j)}^2}}. \qquad [15]$$

Ideal deconvolution leads to $\boldsymbol{P} = +1$ except if there is an even number of antiphase splittings in one dimension, and an odd number in the other, in which case $\boldsymbol{P}$ should reach -1.

Figures 7 and 8 illustrate the efficiency of deconvolution of experimental multiplets taken from a band-selective DQF-COSY spectrum of a cyclopropane derivative:

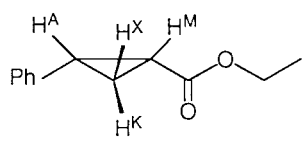

I

The result of deconvolution in both dimensions of the experimental multiplet of Fig. 7a by the antiphase splitting is shown in Fig. 8a. The resulting in-phase multiplet is almost ideal, so that the determination of the in-phase splittings is straightforward.

Figure 9 illustrates deconvolution of another multiplet of the same cyclopropane derivative. In this fully automated recursive analysis, only symmetry was used as a criterion of simplification.

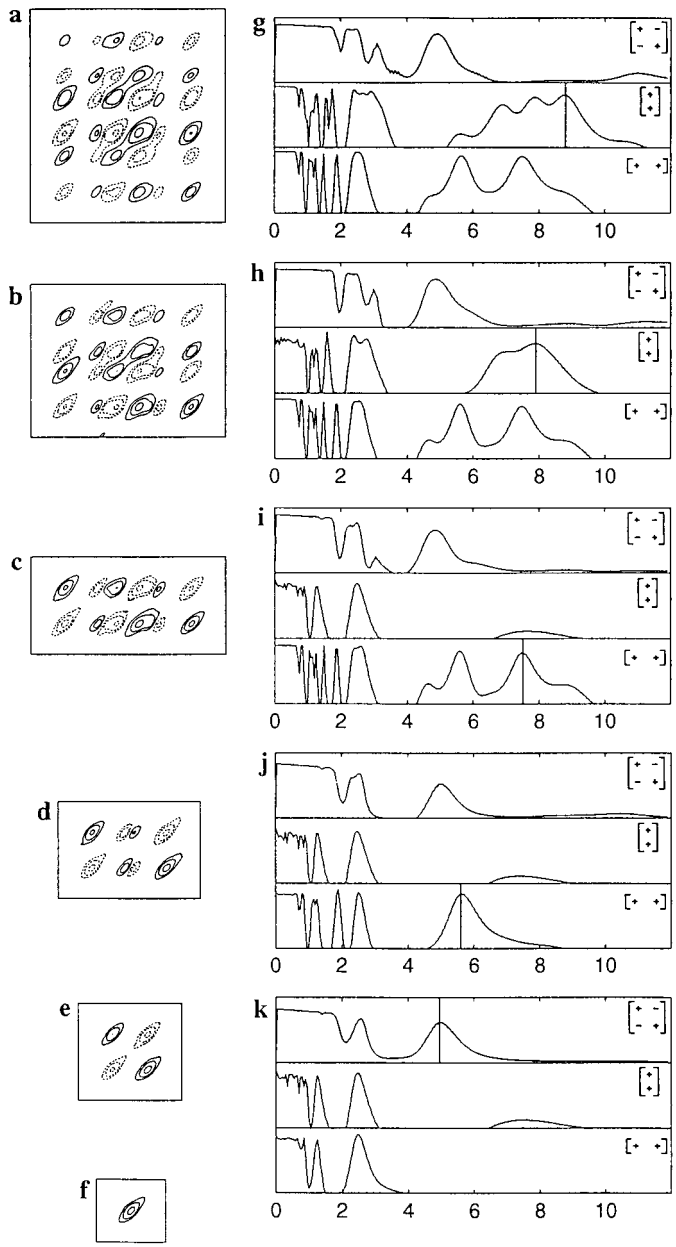

FIG. 9. (a) Experimental multiplet (30 × 28 Hz) stemming from magnetization transfer from X to K in *cis*-2-phenylcyclopropanecarboxylic acid ethyl ester (**I**), taken from a DQF-COSY spectrum with band-selective excitation. (b–f) Recursive simplification obtained by deconvolution. (g–k) Measure of symmetry after deconvolution with an antiphase square (top third of each frame), with a passive in-phase doublet in the vertical ω_1 domain (middle third), and with an in-phase doublet in the horizontal ω_2 dimension (bottom third). The vertical lines indicate extrema corresponding to splittings used in the following deconvolution step. The passive splittings correspond to 8.80 ± 0.05 Hz (g) and 7.90 ± 0.10 Hz (h) in the vertical ω_1 dimension, and to 7.50 ± 0.05 Hz (i) and 5.60 ± 0.05 Hz (j) in the horizontal ω_2 dimension. The active splitting (k) is 4.95 ± 0.05 Hz.

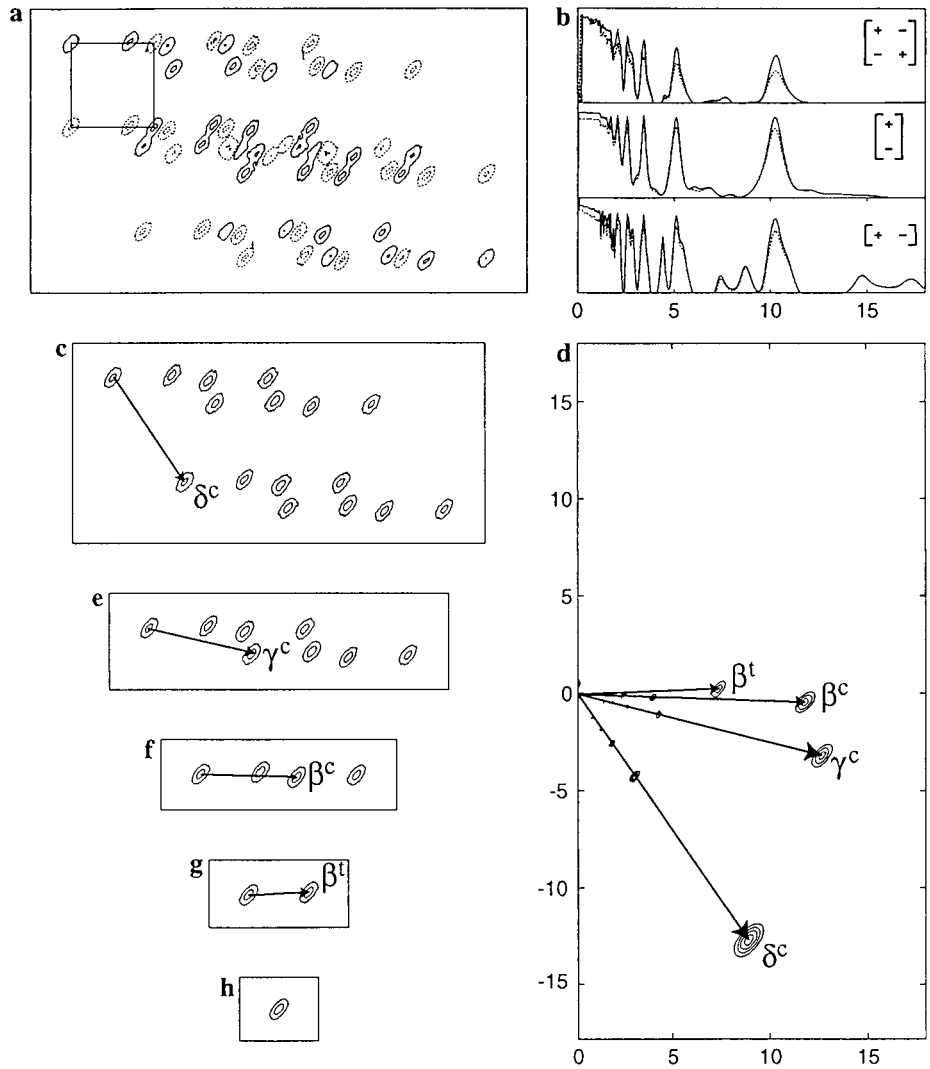

FIG. 10. (a) Soft-COSY multiplet (35 × 61 Hz) correlating the δ^t and γ^t protons (in the vertical ω_1 and horizontal ω_2 dimensions, respectively) of proline[3] in *cyclo*-(L-Pro[1]-L-Pro[2]-D-Pro[3]) (**II**), symmetrized with respect to its C_2 axis. (b) Measure of symmetry after deconvolution with an antiphase square (top third), with an antiphase doublet in the vertical ω_1 dimensions (middle third), and with an antiphase doublet in the horizontal ω_2 dimension (bottom third). The dotted lines correspond to a deconvolution of the raw multiplet (not shown), while the continuous lines result from deconvolution of the C_2-symmetrized multiplet. All six functions give an active coupling constant of 10.25 Hz. (c) Multiplet after deconvolution of the active coupling, symmetrized with respect to its C_2 axis. (d) Two-dimensional map of the measure of symmetry after deconvolution of the passive splittings. The arrows indicate the positions of the minima due to various displacement vectors. Note the presence of local minima at submultiples of the displacement vectors. The contours were taken at 0.4, 0.5, 0.6, and 0.7. (e–h) Successive deconvolution of the splittings due to the spins δ^c, γ^c, β^c, and β^t, followed after each step by C_2 symmetrization. Contours are drawn at ±20 and ±70% of the maximum peak height. In addition to the coupling constants indicated in the coupling network (**II**) one can determine small ^4J splittings $J(\delta^t, \beta^c) = -0.50$ Hz and $J(\delta^t, \beta^t) = 0.45$ Hz. The uncertainty was 0.05 Hz.

When scanned from the right-hand side, the maxima of the uppermost functions in Figs. 9g–9k that are higher than 0.5 are used in the next step of deconvolution. If no maxima are found for $J^* > 0.5$ Hz, the process is stopped. The result is the single peak of Fig. 9f. In the vertical dimension, the multiplet structure is so simple that one could determine the splittings by visual inspection. In the horizontal dimension, on the other hand, cancellation makes such estimates hazardous. Deconvolution deals with both cases equally well.

In soft-COSY multiplets, two independent variables must be determined for each passive spin, corresponding to the ω_1 and ω_2 components of the displacement vector. In order to speed up computation, deconvolution is carried out in two consecutive steps. A first search is made at low resolution (in steps of 0.3 Hz) over a range $-18 < J^* < 18$ Hz in ω_1 and $0 < J^* < 18$ Hz in ω_2, followed by a refinement in steps of 0.05 Hz in the vicinity of the extrema after the digital resolution has been enhanced by trigonometric interpolation. Soft-COSY multiplets are less likely to suffer from cancellation effects than DQF-COSY multiplets. This means that one may deviate from the rule requiring one to search for the largest coupling first. We therefore propose to start with the deconvolution of the

active coupling in both dimensions, and then search for passive splittings in the simplified multiplet.

This methodology is applied to a challenging soft-COSY multiplet extracted from a spectrum of D-Pro[3] of *cyclo*-(L-Pro[1]-L-Pro[2]-D-Pro[3]) (*18*) with the following coupling network:

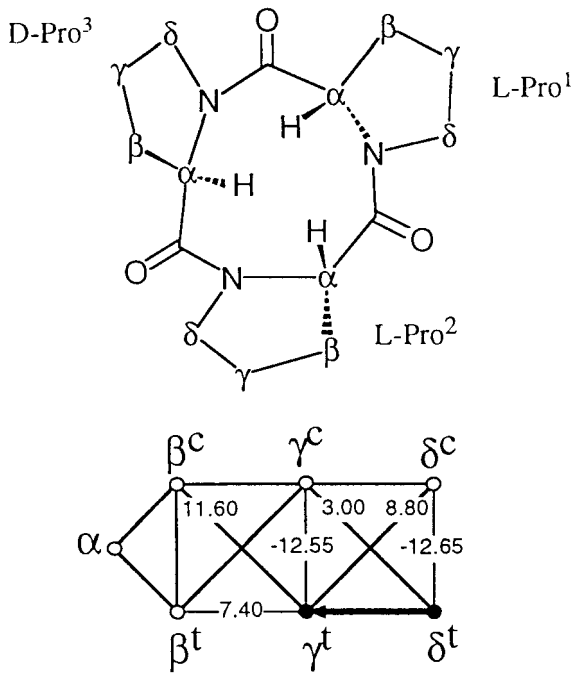

II

The determination of the active coupling, shown in Fig. 10b, can be achieved successfully using any one of three criteria. Symmetrization of the raw multiplet has a beneficial effect for all criteria (from dashed to continuous lines in Fig. 10b). Two-dimensional deconvolution (top frame in Fig. 10b) gives maxima that are less well defined because the imperfections in both dimensions tend to add up. Successive steps of one-dimensional deconvolution (middle and bottom frames in Fig. 10b) provide more pronounced extrema.

In an earlier publication (*19*), we applied deconvolution to 14 soft-COSY multiplets of Paclitaxel (Taxol) and compared results with those of convolution methods (*20, 21*). It turns out that deconvolution is very effective in measuring small splittings and can be applied to all E-COSY type structures. A discussion of small splitting in DQF-COSY multiplets is given elsewhere (*8*).

In conclusion, frequency-domain deconvolution appears to be an effective tool for analyzing multiplets containing both antiphase and in-phase splittings. The method is robust enough to allow fully automatic analysis of complex structures.

ACKNOWLEDGMENTS

This work has been supported by the Commission pour la Technologie et l'Innovation and by the Fonds National de la Recherche Scientifique, both of Switzerland, and by the National High Magnetic Field Laboratory in Tallahassee, Florida.

REFERENCES

1. L. McIntyre and R. Freeman, Accurate measurement of coupling constants by *J* doubling, *J. Magn. Reson.* **96,** 425 (1992).
2. J.-M. Le Parco, L. McIntyre, and R. Freeman, Accurate coupling constants from two-dimensional correlation spectra by "*J* deconvolution," *J. Magn. Reson.* **97,** 553 (1992).
3. L. McIntyre and R. Freeman, Fine structure in NMR correlation spectroscopy, *Isr. J. Chem.* **32,** 231 (1992).
4. M. A. Delsuc and G. C. Levy, The application of maximum entropy processing to the deconvolution of coupling patterns in NMR, *J. Magn. Reson.* **76,** 306 (1988).
5. M. J. Seddon, A. G. Ferrige, P. N. Sanderson, and J. C. Lindon, Automatic recognition of multiplet patterns and measurement of coupling constants in NMR and EPR spectra through the application of maximum-entropy deconvolution, *J. Magn. Reson. A.* **119,** 191 (1996).
6. J. A. Jones, D. S. Grainger, P. J. Hore, and G. J. Daniel, Analysis of COSY cross peaks by deconvolution of the active splittings, *J. Magn. Reson. A* **101,** 162 (1993).
7. J. Stonehouse and J. Keeler, A convenient and accurate method for the measurement of the values of spin–spin coupling constants, *J. Magn. Reson. A* **112,** 43 (1995).
8. D. Jeannerat, "Progress in Cross-Peak Structure Analysis in Two-Dimensional Nuclear Magnetic Resonance Spectroscopy," Ph.D. thesis, Lausanne (1997).
9. P. Huber and G. Bodenhausen, Simplification of multiplets by deconvolution in one- and two-dimensional NMR spectra, *J. Magn. Reson. A* **102,** 81 (1993).
10. R. N. Bracewell, "The Fourier Transform and Its Applications," McGraw–Hill, New York (1978).
11. P. Huber and G. Bodenhausen, Bidirectional deconvolution, an improvement for the stepwise simplification of multiplets, *J. Magn. Reson. A* **104,** 96 (1993).
12. A. A. Bothner-By, Private communication (1995).
13. D. Jeannerat and U. Burger, Application of frequency domain deconvolution to DQF-COSY spectra for the determination of coupling constants as a tool for signal assignment based on coupling networks, submitted for publication.
14. U. Piantini, O. W. Sørensen, and R. R. Ernst, Multiple quantum filters for elucidating NMR coupling networks, *J. Am. Chem. Soc.* **104,** 6800 (1982).
15. A. J. Shaka and R. Freeman, Simplification of NMR spectra by filtration through multiple-quantum coherence, *J. Magn. Reson.* **51,** 169 (1983).
16. J. Cavanagh, J. P. Waltho, and J. Keeler, Semiselective two-dimensional NMR experiments, *J. Magn. Reson.* **74,** 386 (1987).
17. B. U. Meier and R. R. Ernst, Cross-peak analysis in 2D NMR spectroscopy by recursive multiplet contraction, *J. Magn. Reson.* **79,** 540 (1988).
18. H. Kessler, W. Bermel, A. Friedrich, G. Krack, and W. E. Hull, Peptide conformation. 17. *cyclo*-(L-Pro-L-Pro-D-Pro). Conformational analysis by 270- and 500-MHz one- and two-dimensional ^{1}H NMR spectroscopy, *J. Am. Chem. Soc.* **104,** 6297 (1982).
19. C. Peng, D. Jeannerat, and G. Bodenhausen, Determination of homonuclear coupling constants by combining selective two-dimensional NMR spectroscopy with convolution and deconvolution: Application to Paclitaxel (Taxol), *Magn. Reson. Chem.* **35,** 91 (1997).
20. D. Jeannerat and G. Bodenhausen, Determination of active scalar coupling constants by two-dimensional convolution of complementary cross-peak multiplets, *J. Magn. Reson.* **117,** 123 (1995).
21. D. Jeannerat and G. Bodenhausen, Accurate determination of passive coupling constants by analysis of complementary two-dimensional cross-peak multiplets, *J. Magn. Reson. A* **118,** 126 (1996).